Human Molecular Genetics, 2013, Vol. 22, No. 9 **1746–1754**
doi:10.1093/hmg/ddt021
Advance Access published on January 28, 2013

Missense mutations in β-1,3-*N*-acetylglucosaminyltransferase 1 (*B3GNT1*) cause Walker–Warburg syndrome

Karen Buysse[1,†], Moniek Riemersma[1,2,†], Gareth Powell[4,†], Jeroen van Reeuwijk[1,†], David Chitayat[5,6,†], Tony Roscioli[1,7], Erik-Jan Kamsteeg[1], Christa van den Elzen[1], Ellen van Beusekom[1], Susan Blaser[8], Riyana Babul-Hirji[6], William Halliday[5,6], Gavin J. Wright[4], Derek L. Stemple[4], Yung-Yao Lin[4,9], Dirk J. Lefeber[2] and Hans van Bokhoven[1,3,*]

[1]Department of Human Genetics, Nijmegen Centre for Molecular Life Sciences, [2]Department of Neurology, Department of Laboratory Medicine, Institute for Genetic and Metabolic Disease, [3]Department of Cognitive Neurosciences, Donders Institute for Brain, Cognition and Behaviour, Radboud University Nijmegen, 6525 GA Nijmegen, the Netherlands, [4]Wellcome Trust Sanger Institute, Wellcome Trust Genome Campus, Hinxton, Cambridge CB10 1SA, UK, [5]Mount Sinai Hospital, The Prenatal Diagnosis and Medical Genetics Program, Department of Obstetrics and Gynecology, University of Toronto, M5G 1Z5 Toronto, Canada, [6]The Hospital for Sick Children, Division of Clinical and Metabolic Genetics, M5G 1X8 Toronto, Canada, [7]School of Women's and Children's Health, Sydney Children's Hospital and the University of New South Wales, Sydney, New South Wales, Australia, [8]The Hospital for Sick Children, Division of Neuroradiology, M5G 1X8 Toronto, Canada and [9]Blizard Institute, Barts and The London School of Medicine and Dentistry, Queen Mary University of London, Newark Street, London E1 2AT, UK

Received November 22, 2012; Revised and Accepted January 18, 2013

Several known or putative glycosyltransferases are required for the synthesis of laminin-binding glycans on alpha-dystroglycan (αDG), including POMT1, POMT2, POMGnT1, LARGE, Fukutin, FKRP, ISPD and GTDC2. Mutations in these glycosyltransferase genes result in defective αDG glycosylation and reduced ligand binding by αDG causing a clinically heterogeneous group of congenital muscular dystrophies, commonly referred to as dystroglycanopathies. The most severe clinical form, Walker–Warburg syndrome (WWS), is characterized by congenital muscular dystrophy and severe neurological and ophthalmological defects. Here, we report two homozygous missense mutations in the β-1,3-*N*-acetylglucosaminyltransferase 1 (*B3GNT1*) gene in a family affected with WWS. Functional studies confirmed the pathogenicity of the mutations. First, expression of wild-type but not mutant *B3GNT1* in human prostate cancer (PC3) cells led to increased levels of αDG glycosylation. Second, morpholino knockdown of the zebrafish *b3gnt1* orthologue caused characteristic muscular defects and reduced αDG glycosylation. These functional studies identify an important role of B3GNT1 in the synthesis of the uncharacterized laminin-binding glycan of αDG and implicate *B3GNT1* as a novel causative gene for WWS.

INTRODUCTION

Dystroglycanopathies are caused by reduced glycosylation of alpha-dystroglycan (αDG) (1,2). This group of muscular dystrophy-dystroglycanopathy syndromes includes a range of clinical phenotypes. Walker–Warburg syndrome (WWS; MIM 236 670), muscle–eye–brain disease (MEB; MIM 253 280) and Fukuyama congenital muscular dystrophy

*To whom correspondence should be addressed at: Department of Human Genetics 855, Radboud University Nijmegen Medical Centre, Nijmegen, PO Box 9101, 6500 HB Nijmegen, the Netherlands. Tel: +31243616696; Fax: +31243668752; Email: h.vanbokhoven@gen.umcn.nl
†The authors wish it to be known that, in their opinion, the first five authors should be regarded as joint First Authors.

(FCMD; MIM 253 800) represent the most severe end of the clinical spectrum. These disorders cause muscular dystrophy and severe eye and brain abnormalities resulting in early infantile death (3). The mildest variant of the dystroglycanopathies is adult-onset limb-girdle muscular dystrophy (LGMD; MIM 607 155), associated with mutations in the fukutin-related protein (*FKRP*) gene (4).

αDG and beta-dystroglycan (βDG) are central components of the dystrophin–glycoprotein complex (DGC), which forms a link between the cytoskeleton and the basal lamina. The peripheral membrane αDG protein is connected to the cytoskeleton via non-covalent binding with the transmembrane βDG protein that is linked to intracellular actin. The link with the basal lamina is formed by the binding of αDG to several tissue-specific extracellular matrix (ECM) proteins, including laminin, agrin, perlecan, neurexin and pikachurin (5–11). αDG is highly glycosylated with N-glycans, mucin type O-glycans and O-mannose type glycans (12–14). αDG–ligand binding requires specific glycosylation of αDG (6) through O-linked mannosylation of serine or threonine residues. The proposed ligand-binding glycan occurs on a phosphodiester-linked O-mannose residue (15).

Reduced αDG–ligand binding caused by hypoglycosylation of αDG has been suggested to be the underlying cause for the dystroglycanopathies (1,2). Mutations in *POMT1*, *POMT2*, *POMGNT1*, *LARGE*, *FKTN*, *FKRP, ISPD* and *GTDC2,* encoding known or putative glycosyltransferases, and a mutation in the dystroglycan gene (*DAG*) itself give rise to dystroglycanopathies with specific O-glycosylation defects (4,16–23). Furthermore, the phenotypes of patients with mutations in genes involved in producing the sugar precursor dolichol-phosphate mannose (*DOLK*, *DPM3, DPM2* and likely *DPM1*) are associated with dystroglycanopathies with combined N- and O-linked glycosylation defects (24–26). The mannose group of dolichol-phosphate mannose is used during the first step of the O-mannosylation of αDG by an O-mannosyltransferase complex that is encoded by *POMT1* and *POMT2* (27). Protein O-linked-mannose β-1,2-*N*-acetylglucosaminyltransferase 1 (POMGnT1) is involved in the second step of the O-mannosylation. This enzyme adds an *N*-acetylglucosamine residue to the first mannose (18). The exact functions of the proteins encoded by *FKTN, FKRP, ISPD* and *GTDC2* are still unknown. However, the protein products of these genes might play a role in the glycosylation of the phosphorylated O-mannose glycan (15). LARGE has been shown to act as a bifunctional glycosyltransferase that transfers both xylose and glucuronic acid. These glycan modifications allow αDG to bind ECM ligands (28). Recently, a mutation was identified in the *DAG1* gene, which encodes the dystroglycan precursor protein that is post-transcriptionally cleaved into αDG and βDG (29). This mutation, identified in a patient with an LGMD phenotype, interfered with post-translational modifications involving LARGE (30).

Mutation analysis of all known dystroglycanopathy genes has revealed the underlying genetic aetiology in ∼50% of individuals from our cohort of patients with a severe dystroglycanopathy phenotype, suggesting that more genes remain to be discovered. The identification of new genes is important to increase insights into the nature of the unknown ligand-binding glycan. This study provides the first evidence that mutations in β-1,3-*N*-acetylglucosaminyltransferase 1 (*B3GNT1*) can give rise to WWS.

RESULTS

Homozygosity mapping and *B3GNT1* mutation analysis

To identify causative mutations for WWS, we previously performed homozygosity mapping in 30 families with idiopathic WWS using the Affymetrix GeneChip Human Mapping SNP Array (21). Eight families showed homozygosity at 11q13, containing the *B3GNT1* gene, which was associated with αDG glycosylation before in a cellular model of prostate cancer (31). For this reason, we followed a candidate gene approach and focused on *B3GNT1* in our cohort. In one of these families (WWS-31), the homozygous region was delimited by SNP_A-4215126 at 11q13.1 and SNP_A-2154685 at 11q13.3 (UCSC hg19 database, http://genome.ucsc.edu, last accessed date on 30 January, 2013), representing a 5.24 Mb haplotype that was shared among the three affected individuals but different from that in an unaffected sibling. In this family, we detected two homozygous missense mutations in the coding sequence of *B3GNT1*. No *B3GNT1* mutations were detected in any of the other seven families with homozygosity at 11q13.1, nor in any of the 47 additional families from our dystroglycanopathy cohort. Both mutations are absent in 5379 control samples from the NHLBI GO Exome Sequencing Project (Exome Variant Server, http://evs.gs.washington.edu/EVS, last accessed date on 30 January, 2013) and in 672 exomes of our in-house database.

B3GNT1 is a type II transmembrane protein and both mutations are located in the conserved glycosyltransferase domain (Glyco_transf_49, pfam13896; Fig. 1; Supplementary Material, Fig. S1). The first mutation, c.1168A > G (M1), is predicted to lead to a substitution of asparagine by aspartic acid (p.Asn390Asp), while the second mutation, c.1217C > T (M2), replaces alanine by valine (p.Ala406Val). Screening of all available family members showed co-segregation with disease, with all affected members being homozygous and all unaffected individuals being heterozygous for both the mutations (Supplementary Material, Fig. S2).

Clinical report

The index family (WWS-31) without known consanguinity is of East Indian descent with four siblings diagnosed with WWS and three unaffected sibs (Fig. 1E) (clinical details are described in the Materials and Methods section). Three pregnancies were terminated and one affected son died at 2 years of age. He presented with hydrocephalus, Dandy–Walker malformation, retinal dysplasia, severe hypotonia and seizures. His creatine kinase (CK) level was very high (3180 units/l). The magnetic resonance imaging (MRI, Fig. 2A–D) showed typical WWS characteristics such as ventricular enlargement, diffuse widening of the gyri and disorganization of the cortical sulci with areas of cobblestone lissencephaly along the posterior aspects of the occipital lobes and temporal lobes. Besides, the white matter, brain stem and cerebellum were clearly affected. From one of the fetuses, a muscle biopsy was taken. The skeletal muscle

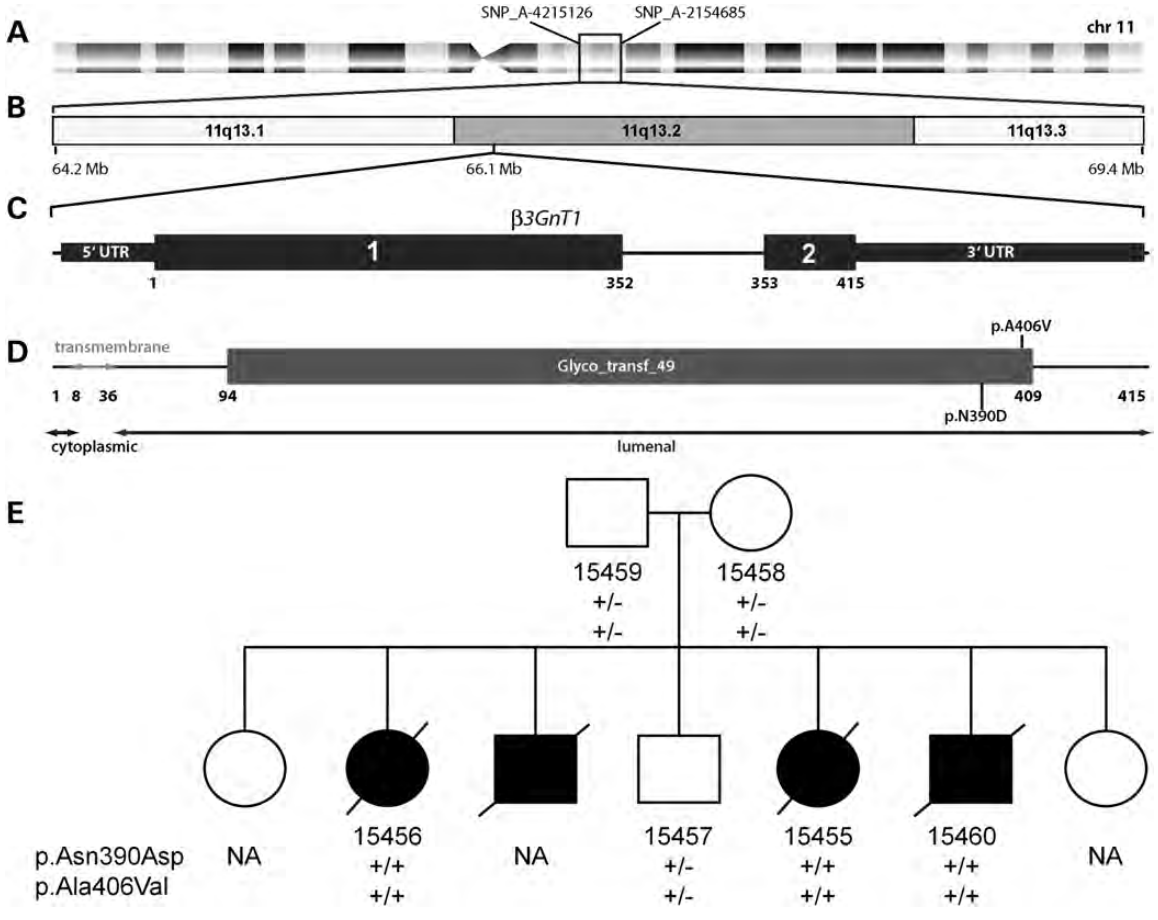

Figure 1. Schematic representation of *B3GNT1* chromosomal position, protein structure and localization of mutations. (**A**) Ideogram of chromosome 11 showing the localization of the SNPs flanking the shared homozygous region in the patients. (**B**) Zoom-in of the 5.2 Mb homozygous region. (**C**) Gene structure of *B3GNT1* showing the 5′ UTR, two coding exons separated by the intron and the 3′ UTR. (**D**) Protein structure of B3GNT1 showing the topological domains, the conserved glycosyltransferase domain and the position of the missense mutations M1 (p.N390D) and M2 (p.A406V). (**E**) Pedigree of family WWS-31. Individuals that were available for study are identified by their lab number. The mutation status is indicated below each individual (+, present, −, absent, NA, not available).

showed a lack of merosin and α-sarcoglycan expression. In addition, αDG was not able to bind laminin as assessed by laminin overlay in skeletal muscle homogenate (Fig. 2E).

Overexpression of wild-type and mutant *B3GNT1* in human PC3 cells

To investigate the functional consequences of the mutations, we first determined the subcellular localization of wild-type and mutant B3GNT1. We used human prostate cancer (PC3) cells with low levels of endogenous αDG glycosylation (31). We transfected PC3 cells with enhanced green fluorescent protein (EGFP)-tagged wild-type and mutant *B3GNT1* constructs. Wild-type and single or double mutant fusion proteins localized to the Golgi apparatus of transfected cells, as determined by co-localization with the Golgi marker Giantin (GOLGB1, Fig. 3). These results show that the mutations do not affect B3GNT1 subcellular localization.

To investigate the effect of wild-type and mutant forms of *B3GNT1* on αDG glycosylation, a flow cytometry assay was performed using the IIH6 antibody directed against glycosylated αDG (1). The number of IIH6-positive cells strongly increased on transfection with wild-type *B3GNT1* when compared with transfection with an empty vector. Transfection with single mutants and the double mutant did not cause an increase of IIH6-positive cells. Normalization of the results as percentage of IIH6-positive cells in relation to the empty vector control showed a statistically significant difference in αDG glycosylation between wild-type and mutant constructs (Fig. 4; $P = 0.042$). These results indicate that the identified mutations impair the glycosyltransferase function of B3GNT1.

Morpholino knockdown of zebrafish *b3gnt1*

To evaluate the phenotypic consequences of loss of function of B3GNT1 *in vivo*, we used zebrafish embryos as a model for the dystroglycanopathies (21). The zebrafish ortholog, B3gnt1, shows 67% similarity to the human B3GNT1 protein sequence, including conservation of the two amino acid residues mutated in the family affected by WWS: Asn390 and Ala406 (Supplementary Material, Fig. S1).

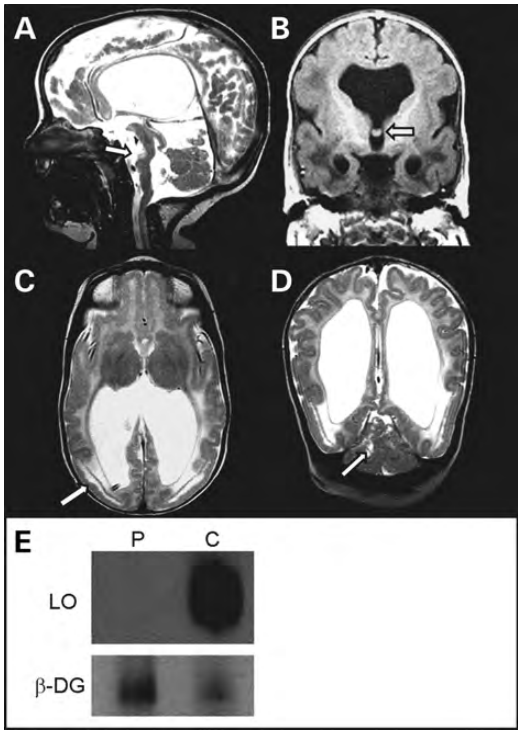

Figure 2. (**A**–**D**) MRI at 4 months of age. Sagittal T2W image (**A**) reveals hydrocephalus, a hypoplastic 'Z'-shaped brainstem (arrow) and a hypoplastic, dysplastic vermis. Coronal T1W image (**B**) demonstrates absence of the septal leaflets, vertical hippocampi and fusion of the forniceal columns in the midline (arrow). Axial T2W image (**C**) shows focal cobblestone lissencephaly of the occipital cortex (arrow). The subjacent white matter is abnormally increased in signal intensity. A shunt is present in the posterior horn of the right lateral ventricle. In addition to ventriculomegaly and focal cobblestone lissencephaly, coronal T2W image (**D**) reveals cysts (arrow) within the dysplastic cerebellum. (**E**) Patient (P) and control (C) muscle homogenates were used for a laminin overlay assay (LO). β-Dystroglycan (β-DG) staining was used as loading control.

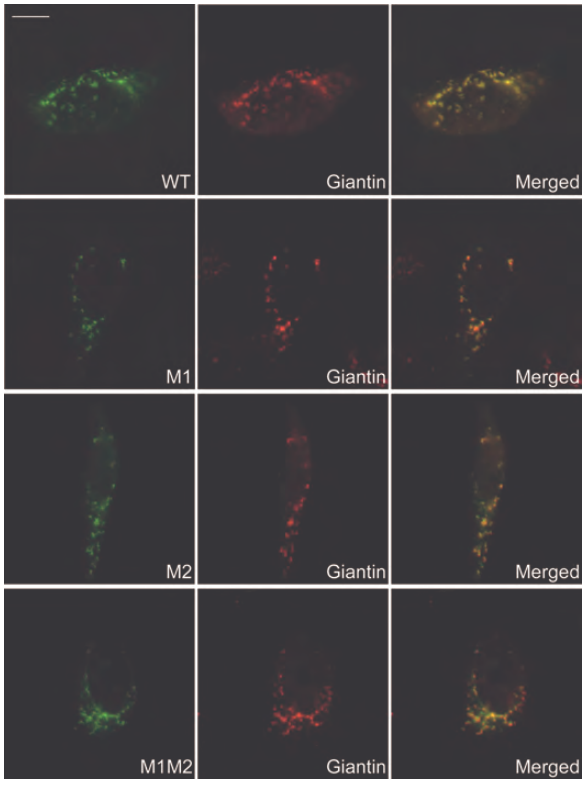

Figure 3. Cellular localization of wild-type and mutant B3GNT1. Wild-type and mutant variants of EGFP-tagged B3GNT1 (green) colocalize with the Golgi marker Giantin (red). Scale bar represents 10 μm.

RT-PCR analysis showed that *b3gnt1* is expressed in wild-type embryos throughout the first five days of development (Fig. 5A). To knockdown *b3gnt1*, we injected zebrafish embryos with a morpholino designed to disrupt splicing of the only intron in the *b3gnt1* gene (Fig. 1C). We observed a great reduction in the expression of the full-length transcript and the appearance of aberrantly spliced transcripts by RT-PCR (Fig. 5B), using complementary DNA (cDNA) extracted from 48 h post fertilization (hpf) morphant embryos.

To assess the effect of loss of function of B3gnt1 on glycosylation of αDG, we extracted cell surface proteins from 48 hpf uninjected (positive control), *b3gnt1* morpholino-treated and *dag1* morpholino-treated (negative control) embryos. We tested the protein extracts for the presence of laminin-binding glyco-epitopes by western blot, using the IIH6 antibody (Fig. 5C). Little or no glycosylated αDG was observed in extracts from *b3gnt1* morphants compared to wild-type. These results demonstrate that loss of function of B3gnt1 results in hypoglycosylation (Fig. 5C) and verifies the efficacy of the morpholino.

To investigate the effect of *b3gnt1* morpholino knockdown on the muscle fibre structure and organization, we stained 48 hpf morphant and control embryos with phalloidin, which labels filamentous actin (F-actin) and an antibody against βDG to label myotendinous junctions (MTJs). Muscle fibre organization and structure were disrupted in morphant embryos (Fig. 5D), including muscle fibre detachment and discontinuous MTJs, with elongated muscle fibres spanning the myosepta. Sarcolemma integrity was evaluated by injection of Evan's blue dye (EBD), which only penetrates the cell when the membrane is compromised (Fig. 5E). Accumulation of EBD was observed in the muscle lesions, indicating muscle degeneration with a loss of sarcolemma integrity in *b3gnt1* morphant embryos.

Taken together, these results demonstrate that the missense mutations in *B3GNT1* in this WWS family significantly impair its function *in vitro* as well as *in vivo* in zebrafish, showing a muscle phenotype comparable with dystroglycanopathy.

DISCUSSION

Dystroglycanopathies are caused by mutations in (putative) glycosyltransferases and sugar donors that result in aberrant glycosylation of αDG. Identification of all genes involved is essential for understanding the pathology in this group of disorders with abnormal glycosylation of the αDG glycan. In this study, we identified two missense mutations in *B3GNT1* in a family affected with WWS and showed that these mutations are causative for the disease. First, the mutations reside in the conserved glycosyltransferase domain, show complete segregation with the disease in the index family and are absent in

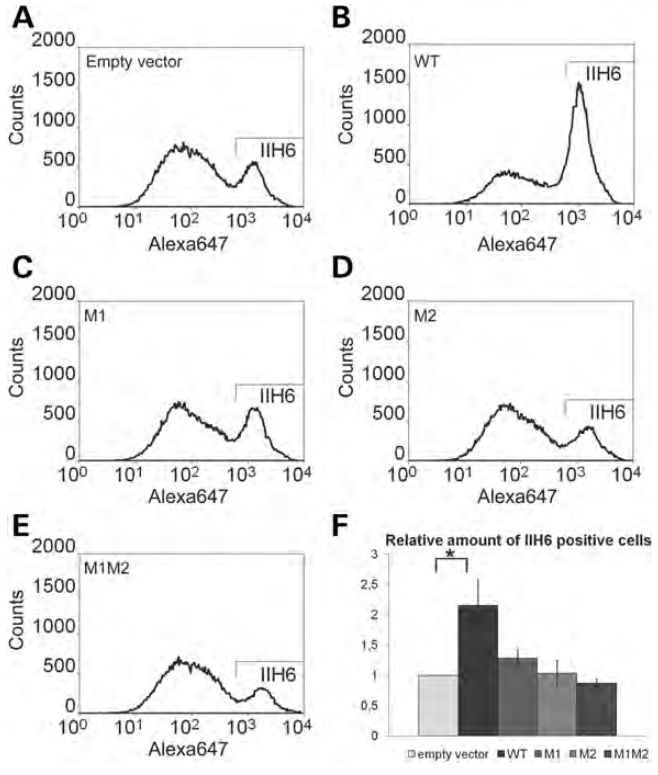

Figure 4. Flow cytometry analysis of transfected PC3 cells. PC3 cells transfected with an empty vector are used as control (**A**). In *B3GNT1* WT transfected PC3 cells (**B**) the percentage of IIH6-positive cells is significantly higher than in PC3 cells transfected with an empty vector (A, F). The percentages of IIH6-positive cells in B3GNT1 M1 (**C**), B3GNT1 M2 (**D**) and B3GNT1 M1M2 (E) transfected PC3 cells are comparable with the percentage of the PC3 cells transfected with the empty vector (A, summary in **F**), indicating that glycosylation is affected. (F) Bar chart showing the relative amount of IIH6-positive cells, taking the empty vector control as standard ($n = 3$, $^*P < 0.05$, one sample *T*-test). Error bars show the standard deviation.

control cohorts. Second, *B3GNT1* overexpression in human PC3 cells results in a significant increase in αDG glycosylation, whereas overexpression of singly or doubly mutated *B3GNT1* is comparable with the negative control. This demonstrates the involvement of B3GNT1 in αDG glycosylation and the pathogenicity of the missense mutations. Third, morpholino knockdown of the zebrafish ortholog *b3gnt1* results in phenotypic features that are reminiscent of WWS, with muscle structure disorganization being the most prominent finding. Taken together, these results indicate that B3GNT1 is required for the interaction between αDG and laminin, as impaired B3GNT1 function leads to diminished glycosylation and subsequent disruption of ligand binding, leading to phenotypic WWS features. Previous genetic analyses in patients with mild-end dystroglycanopathy phenotypes have not revealed *B3GNT1* mutations (32). Furthermore, we have identified only one family in our cohort of WWS patients, suggesting that it is a rare cause of dystroglycanopathies. One hypothesis is that more severe mutations might cause embryonic lethality and have hitherto remained undetected.

The exact function of B3GNT1 in αDG O-mannosylation is still unknown. *B3GNT1* is expressed in tissues typically affected in dystroglycanopathies, including skeletal muscle and brain (33). Previous studies in a prostate cancer cell line (28) indicated a role of B3GNT1 in the synthesis of the laminin-binding glycan. B3GNT1 was originally characterized as an enzyme involved in the formation of poly-*N*-acetyllactosamine glycans by adding *N*-acetylglucosamine residues to *N*-acetyllactosamines attached to N-glycans (33). It has been proposed that B3GNT1 forms a complex with LARGE and that terminal *N*-acetylglucosamine residues are targets for LARGE glycosyltransferase activity (31,34). One possibility is that B3GNT1 adds a terminal *N*-acetylglucosamine residue to the phosphodiester-linked glycan that acts as an acceptor for LARGE activity. A recent study has shown that LARGE transfers both xylose and glucuronic acid residues to the unknown ligand-binding glycan (28), perhaps using the *N*-acetylglucosamine residue transferred by B3GNT1 as initiating sugar. It is not yet known how these xylose and glucuronic acid structures contribute to ligand binding. Together with previous studies, our data suggest that at least three *N*-acetylglucosaminyl transferases with different specificities are required for synthesis of the ligand-binding glycan on αDG. POMGnT1 is responsible for addition of an *N*-acetylglucosamine residue in β-1,2 linkage to the first mannose residue. However, the *N*-acetylglucosamine residue in the phosphodiester-linked O-mannose trisaccharide was proposed in the β-1,4 linkage, while B3GNT1 is supposed to add an *N*-acetylglucosamine residue in the β-1,3 linkage, likely in the post-phosphoryl glycan (15,33). Altogether, the synthesis of the laminin-binding glycan on αDG still remains unclear, necessitating further mechanistic studies to position uncharacterized proteins as FKRP, FKTN, GTDC2 and ISPD in the pathway (15,21).

In conclusion, we have detected two pathogenic missense mutations in *B3GNT1* which result in impaired glycosylation of αDG, giving rise to WWS. Our genetic and functional data provide evidence that *B3GNT1* is a novel causative gene for the dystroglycanopathies and recommend its inclusion in the diagnostic workup of patients.

MATERIALS AND METHODS

Clinical report

The index family (WWS-31) is a non-consanguineous family of East Indian descent with four affected children and three unaffected siblings (Fig. 1E). The mother had a history of gestational diabetes. The remainder of the family history is noncontributory for additional risk factors. The couple's first pregnancy, when the parents were 25 years old, resulted in a daughter who is well.

The second pregnancy was complicated with fetal ultrasound findings, at 22 weeks of gestation, of hydrocephalus with the lateral ventricles measuring 24 mm each and the third ventricle measuring 5 mm. The cerebellum and brainstem were hypoplastic. The pregnancy was terminated at 24.9 weeks gestation and the autopsy showed diffuse and severe leptomeningeal neuroepithelial heterotopia, maximal over the convexity of the cerebral hemispheres and ventral brainstem. There was obliteration of the subarachnoid space and diffuse communicating hydrocephalus. There was severe dysplasia/hypoplasia of the cerebellar hemisphere and

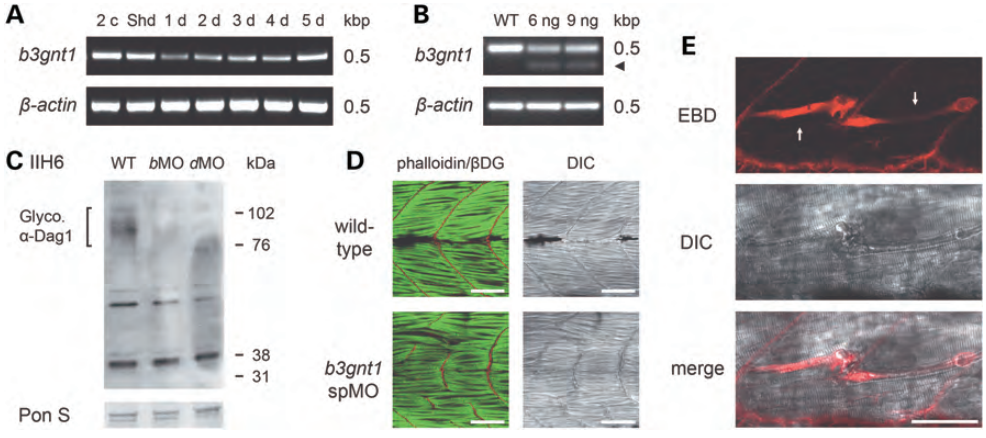

Figure 5. Knockdown of zebrafish *b3gnt1* causes muscle defects and reduced glycosylation of αDG. (A and B) RT-PCR results showing that *b3gnt1* is expressed throughout zebrafish embryonic development (**A**) but greatly reduced in 48 hpf embryos treated with 6 ng or 9 ng of *b3gnt1* morpholino (2c, two-cell stage; Shd, shield stage; d, days post fertilization) (**B**), compared with β-actin loading control; arrow indicates aberrantly spliced *b3gnt1* transcripts. (**C**) Western blot using IIH6 antibody to detect the αDG glycosylation state (Glyco. αDag1) in 48 hpf wild-type (wt), *b3gnt1* morphant (bMO) or *dag1* morphant (dMO) embryos. Knockdown of *b3gnt1* causes hypoglycosylation of αDG compared with wild-type. Ponceau staining (PonS) loading control shown below. (**D**) Fluorescent confocal microscopy images of 48 hpf wild-type (top) and *b3gnt1* morphant (bottom) embryos stained with phalloidin (green), and the corresponding DIC images. Loss of function of *b3gnt1* results in disrupted MTJs as indicated by βDG immunoreactivity (red) and muscle fibres spanning multiple segments. (**E**) Compromised sarcolemmal integrity precedes fibre detachment in *b3gnt1* morpholino-treated embryos. Fluorescent confocal microscopy image of a 48 hpf embryo, previously injected with b3gnt1 splice-blocking morpholino, treated with EBD (top panel) to highlight muscle fibres with disrupted sarcolemma (arrows). The corresponding DIC image is shown in the middle panel. Representative images of identified muscle lesions from three independent experiments; scale bar represents 50 μm.

vermis and ventral brainstem hypoplasia, maximal at the basis pontis. The karyotype was normal (46, XX).

The third pregnancy was complicated with cerebral ventriculomegaly involving the lateral and third ventricles with a very thin and smooth cortex at 23 weeks gestation. The cerebellum was hypoplastic and the cisterna magna was enlarged. There was multicystic dysplastic left kidney and very few tiny cysts appeared in the right kidney. The karyotype was normal (46, XY). The couple was counselled and decided to terminate the pregnancy. The autopsy showed a male fetus with a cystic dysplastic left kidney with a thread-like ureter, testicular hypoplasia with decreased number and marked size variation of seminiferous tubules, 12 ribs on the right and 11 on the left and X-ray finding of 'beaten silver' frontal and parietal skull bones. Neuropathological investigation showed lissencephaly type II with cortical dysplasia, severe wavy island architecture and extensive glio-neuroepithelial leptomeningeal heterotopia with obliteration of the subarachnoid space. There was severe communicating hydrocephalus. The cerebellum showed severe cortical dysplasia/hypoplasia with inferior vermian defect. There was hypoplasia of the pyramids at the level of the medulla and the inferior olives had a C-shaped dysplasia. There was hydromyelia. The eyes showed no anterior segmental abnormalities, focal abnormalities involving the retinae of both eyes including the disorganized neuronal layer with irregular nests of neurons in the nerve fibre layer, some of which appeared to break through the inner limiting membrane. There were no abnormalities of the extraocular muscles. The findings were consistent with retinal dysplasia.

The fourth pregnancy resulted in a son who is well.

The fifth pregnancy resulted in a fetus with WWS. The fetal ultrasound at 17.6 weeks gestation showed a slight 'lemon'-shaped head with bilateral ventriculomegaly measuring 14 mm, a small cerebellum and agenesis of the corpus callosum and inferior vermis. A repeat fetal ultrasound at 21.5 weeks gestation showed hydrocephalus with the lateral ventricles measuring 17 mm. The cerebellum was slightly small and there was partial vermian dysgenesis. The couple was counselled and decided to terminate the pregnancy. The autopsy showed a female fetus with findings consistent with WWS including extensive glio-neuroepithelial leptomeningeal heterotopia with obliteration of the subarachnoid space. There was severe communicating hydrocephalus. There was lissencephaly, absent pyramidal tract and agenesis of the corpus callosum. The cerebellum showed severe cortical dysplasia/hypoplasia and aplasia of the vermis.

The couple's sixth pregnancy resulted in a son, who was diagnosed prenatally with WWS. The couple was counselled and decided to continue the pregnancy. The baby was born at term via Cesarean section due to severe cerebral ventriculomegaly. He presented with hydrocephalus, Dandy–Walker malformation, retinal dysplasia, severe hypotonia and intractable seizures. His CK level was very high (3180 units/l) and the MRI (Fig. 2) showed ventricular enlargement, diffuse widening of the gyri and disorganization of the cortical sulci with areas of cobblestone lissencephaly along the posterior aspects of the occipital lobes and temporal lobes. There was white matter abnormality in association with these findings. The brain stem was severely abnormal with wasting of the pons and medulla. The cerebellum was also extremely dysgenetic with cysts, heterotopia and disarray of cortical migration. There was absence of the septum pellucidum and fusion of the forniceal columns in the midline. The globes were apparently intact with thinning of the posterior sclera and retina, consistent with retinal dysplasia. He had a ventriculoperitoneal shunt inserted and died at 2 years of age.

The couple's seventh pregnancy resulted in a daughter who is well.

Patient cohort

A cohort of 55 families with one or more individuals affected with WWS or MEB were included in this study. Informed consent was obtained from all participants. The study was approved by the ethical board of the Radboud University Nijmegen Medical Centre, CMO Regio Arnhem-Nijmegen Approval 2011/155.

Homozygosity mapping

Genotyping analysis of genomic DNA was performed using the Affymetrix GeneChip Human Mapping 10 K 2.0 Array or 250 K *Nsp*I Array. All SNP array experiments were performed and analysed according to the manufacturer's instructions (Affymetrix, Santa Clara, CA, USA). Homozygosity mapping was performed using an in-house algorithm (J.v.R., unpublished data) for analysis of the genotype files generated by the Affymetrix GTC software. The number of contiguous homozygous SNPs required for significance in relation to the degree of consanguinity for each individual was calculated using an algorithm adapted from a previous study (35). Regions of excess homozygosity were identified in affected individuals and compared with haplotypes of unaffected family members where available.

B3GNT1 mutation analysis

Sequencing of the two coding exons of *B3GNT1* (NCBI Reference Sequence NM_006876.2) was performed using the ABI PRISM BigDye Terminator Cycle Sequencing V2.0 Ready Reaction kit and analysed with the ABI PRISM 3730 DNA analyzer (Applied Biosystems, Foster City, CA, USA). Primer sequences and PCR conditions are available upon request.

Molecular cloning and site-directed mutagenesis

Full-length human *B3GNT1* mRNA was obtained from IMAGE cDNA clone 2 988 041 (Source BioScience). The wild-type human-coding sequences were cloned into the Gateway pDONR^{TM}201 vector (Invitrogen). Site-directed mutagenesis using the QuikChange^{TM} Site-Directed Mutagenesis kit (Stratagene) was carried out to introduce the mutations into the constructs. The presence of the mutations was verified by Sanger sequencing. The human c.1168A>G mutation is referred to as mutation 1 (M1). The c.1217C>T mutation is referred to as mutation 2 (M2). Both single (M1 or M2) and double mutant (M1M2) constructs were designed. Wild-type and mutant sequences were subsequently cloned into pCS2+ based expression vectors that were used for mRNA synthesis and transfection.

Accession number

To clone full open reading frame (ORF) zebrafish *b3gnt1*, we carried out RT-PCR using cDNA from 48 hpf embryos with forward and reverse primers, 5′-TCTTTTTTTTGCTATCCAAAC-3′ and 5′-GCATTCATGAGTGTCTCCTTACA-3′. The full ORF zebrafish *b3gnt1* cDNA has been submitted to GenBank (Accession number: KC136354).

Western blotting

For human muscle tissues, proteins were extracted from paraffin-embedded muscle as described (36). Protein samples were used for western blotting followed by a laminin overlay assay and β-dystroglycan staining as described (1,24). Microsome preparation and western blotting using zebrafish embryos were carried out as previously described (21). The primary antibody used in this study was glycosylated α-dystroglycan IIH6 (Millipore, 1:2000).

Cell culture and transfection

Prostate cancer cells (PC3) (a gift from Gerald Verhaegh of the Department of Urology, Radboud University Nijmegen Medical Centre) were cultured in RPMI 1690 medium (Gibco) supplemented with 10% fetal bovine serum (PAA). Cells were transfected using FuGENE® 6 (Roche) according to manufacturer's instructions. The ratio of transfection reagents (μl) to DNA (μg) used was 6:1. Three days after transfection, the cells were used for immunocytochemistry or flow cytometry analysis.

Immunocytochemistry

Transfected and untransfected cells were cultured on glass cover slips. The cells were briefly washed using phosphate buffered saline (PBS), fixed in 3.7% formaldehyde in PBS at room temperature for 10 min, permeabilized using 0.4% Triton X-100 in 3% BSA/PBS at 4°C for 10 min, blocked with 3% BSA/PBS at room temperature for 30 min and subsequently incubated with Giantin antibody (Covance) diluted 1:400 in 3% BSA/PBS at 4°C for 1 hour. Following primary antibody incubation, the cells were briefly washed using PBS and subsequently incubated with Alexa Fluor® 555 Donkey Anti-Rabbit IgG (Molecular Probes) diluted 1:500 in 3% BSA/PBS at 4°C for one and a half hour. Cover slips were embedded in fluorescence mounting medium (DAKO). The cells were analysed using a Zeiss Axio Imager Z1 fluorescence microscope (Carl Zeiss).

Flow cytometry analysis

Cells were washed using PBS and subsequently scraped in cold PBS. The cells were blocked using 20% goat serum in 1% BSA/PBS on ice for 20 min. The cells were incubated with IIH6 antibody (Millipore) 1:25 diluted in 1% BSA/PBS on ice overnight. The cells were washed and subsequently incubated with Alexa Fluor® 647 Goat Anti-Mouse IgG (Molecular Probes) 1:200 diluted in 1% BSA/PBS on ice for 2 hours. The fluorescent signal of secondary antibody was measured using a CyAn flow cytometer (Beckman-Coulter) with 642 nm laser. A total of 75 000 cells were analysed per experiment. Data were analysed using Summit 4.3 software. The percentage of IIH6-positive cells transfected with wild-type

and mutant *B3GNT1* constructs was normalized against the percentage of IIH6-positive cells transfected with the empty vector (Fig. 4F). Statistical significance was determined using one-sample *t*-test ($n = 3$). A *P*-value of <0.05 was considered statistically significant.

Morpholino and EBD injections in zebrafish

Antisense morpholino oligonucleotides (MOs) were obtained from GeneTools. *dag1* MO has been described (37). *b3gnt1* MO (5′-CCTATTCTCCATGTGCTCACCTGGC-3′) was designed to target the *b3gnt1* exon–intron splice site. All MOs were injected into the yolk flow at one-cell stage using a specified dose in the figure legend. As described (38), 0.1% EBD (Sigma) was injected into zebrafish blood circulation at 48 hpf. MO or EBD-injected embryos were fixed using 4% PFA for immunohistochemistry or analysed live under confocal and differential interference contrast (DIC) microscopy.

Zebrafish immunohistochemistry

Immunostaining of fixed zebrafish embryos was performed as described (21). Alexa Fluor-conjugated phalloidin (Molecular Probes; 1:100 dilution) and primary antibody anti-β-Dag1 (Novocastra, 1:50) were used. Alexa Fluor® 488 or 594 conjugated anti-mouse IgG (Molecular Probes; 1:250 dilution) were used as a secondary antibody.

SUPPLEMENTARY MATERIAL

Supplementary Material is available at *HMG* online.

ACKNOWLEDGEMENTS

We would like to thank all patients and their family members for participation in this study. We also thank Jo (Huiqing) Zhou for insightful discussions and support.

Conflict of interest statement. None declared.

FUNDING

This work was supported by the EU FP7 Health Programme (241995 GENCODYS to H.v.B.); the Prinses Beatrix Fund (grant W.OR09-15 to D.L. and H.v.B.); the Hersenstichting Nederland (grant KS 2009(1)-110 to H.v.B.)]; Wellcome Trust (WT 077047/Z/05/Z, WT 077037/Z/05/Z, WT 098051 to D.L.S. and G.J.W.); and the European Molecular Biology Organization (Long-Term Fellowship ALTF 805-2009 to K.B.). Funding to pay the Open Access publication charges for this article was provided by the Wellcome Trust.

REFERENCES

1. Michele, D.E., Barresi, R., Kanagawa, M., Saito, F., Cohn, R.D., Satz, J.S., Dollar, J., Nishino, I., Kelley, R.I., Somer, H. *et al.* (2002) Post-translational disruption of dystroglycan-ligand interactions in congenital muscular dystrophies. *Nature*, **418**, 417–422.
2. Moore, S.A., Saito, F., Chen, J., Michele, D.E., Henry, M.D., Messing, A., Cohn, R.D., Ross-Barta, S.E., Westra, S., Williamson, R.A. *et al.* (2002) Deletion of brain dystroglycan recapitulates aspects of congenital muscular dystrophy. *Nature*, **418**, 422–425.
3. van Reeuwijk, J., Brunner, H.G. and van Bokhoven, H. (2005) Glyc-O-genetics of Walker–Warburg syndrome. *Clin. Genet.*, **67**, 281–289.
4. Brockington, M., Blake, D.J., Prandini, P., Brown, S.C., Torelli, S., Benson, M.A., Ponting, C.P., Estournet, B., Romero, N.B., Mercuri, E. *et al.* (2001) Mutations in the fukutin-related protein gene (FKRP) cause a form of congenital muscular dystrophy with secondary laminin α2 deficiency and abnormal glycosylation of α-dystroglycan. *Am. J. Hum. Genet.*, **69**, 1198–1209.
5. Henry, M.D. and Campbell, K.P. (1996) Dystroglycan: an extracellular matrix receptor linked to the cytoskeleton. *Curr. Opin. Cell Biol.*, **8**, 625–631.
6. Ervasti, J. and Campbell, K. (1993) A role for the dystrophin-glycoprotein complex as a transmembrane linker between laminin and actin. *J. Cell Biol.*, **122**, 809–823.
7. Campanelli, J.T., Roberds, S.L., Campbell, K.P. and Scheller, R.H. (1994) A role for dystrophin-associated glycoproteins and utrophin in agrin-induced AChR clustering. *Cell*, **77**, 663–674.
8. Gee, S.H., Montanaro, F., Lindenbaum, M.H. and Carbonetto, S. (1994) Dystroglycan-α, a dystrophin-associated glycoprotein, is a functional agrin receptor. *Cell*, **77**, 675–686.
9. Peng, H.B., Ali, A.A., Daggett, D.F., Rauvala, H., Hassell, J.R. and Smalheiser, N.R. (1998) The relationship between perlecan and dystroglycan and its implication in the formation of the neuromuscular junction. *Cell Adhes. Commun.*, **5**, 475–489.
10. Sugita, S., Saito, F., Tang, J., Satz, J., Campbell, K. and Südhof, T.C. (2001) A stoichiometric complex of neurexins and dystroglycan in brain. *J. Cell Biol.*, **154**, 435–446.
11. Sato, S., Omori, Y., Katoh, K., Kondo, M., Kanagawa, M., Miyata, K., Funabiki, K., Koyasu, T., Kajimura, N., Miyoshi, T. *et al.* (2008) Pikachurin, a dystroglycan ligand, is essential for photoreceptor ribbon synapse formation. *Nat. Neurosci.*, **11**, 923–931.
12. Holt, K.H., Crosbie, R.H., Venzke, D.P. and Campbell, K.P. (2000) Biosynthesis of dystroglycan: processing of a precursor propeptide. *FEBS Lett.*, **468**, 79–83.
13. Chiba, A., Matsumura, K., Yamada, H., Inazu, T., Shimizu, T., Kusunoki, S., Kanazawa, I., Kobata, A. and Endo, T. (1997) Structures of sialylated O-linked oligosaccharides of bovine peripheral nerve α-dystroglycan. *J. Biol. Chem.*, **272**, 2156–2162.
14. Sasaki, T., Yamada, H., Matsumura, K., Shimizu, T., Kobata, A. and Endo, T. (1998) Detection of O-mannosyl glycans in rabbit skeletal muscle α-dystroglycan. *Biochim. Biophys. Acta.*, **1425**, 599–606.
15. Yoshida-Moriguchi, T., Yu, L., Stalnaker, S.H., Davis, S., Kunz, S., Madson, M., Oldstone, M.B.A., Schachter, H., Wells, L. and Campbell, K.P. (2010) O-Mannosyl phosphorylation of alpha-dystroglycan is required for laminin binding. *Science*, **327**, 88–92.
16. Beltrán-Valero de Bernabé, D., Currier, S., Steinbrecher, A., Celli, J., van Beusekom, E., van der Zwaag, B., Kayserili, H., Merlini, L., Chitayat, D., Dobyns, W.B. *et al.* (2002) Mutations in the O-mannosyltransferase gene POMT1 give rise to the severe neuronal migration disorder Walker–Warburg syndrome. *Am. J. Hum. Genet.*, **71**, 1033–1043.
17. van Reeuwijk, J., Janssen, M., van den Elzen, C., Beltrán-Valero de Bernabé, D., Sabatelli, P., Merlini, L., Boon, M., Scheffer, H., Brockington, M., Muntoni, F. *et al.* (2005) POMT2 mutations cause α-dystroglycan hypoglycosylation and Walker–Warburg syndrome. *J. Med. Genet.*, **42**, 907–912.
18. Yoshida, A., Kobayashi, K., Manya, H., Taniguchi, K., Kano, H., Mizuno, M., Inazu, T., Mitsuhashi, H., Takahashi, S., Takeuchi, M. *et al.* (2001) Muscular dystrophy and neuronal migration disorder caused by mutations in a glycosyltransferase, POMGnT1. *Dev. Cell*, **1**, 717–724.
19. Longman, C., Brockington, M., Torelli, S., Jimenez-Mallebrera, C., Kennedy, C., Khalil, N., Feng, L., Saran, R.K., Voit, T., Merlini, L. *et al.* (2003) Mutations in the human LARGE gene cause MDC1D, a novel form of congenital muscular dystrophy with severe mental retardation and abnormal glycosylation of α-dystroglycan. *Hum. Mol. Genet.*, **12**, 2853–2861.
20. Kobayashi, K., Nakahori, Y., Miyake, M., Matsumura, K., Kondo-Iida, E., Nomura, Y., Segawa, M., Yoshioka, M., Saito, K., Osawa, M. *et al.* (1998) An ancient retrotransposal insertion causes Fukuyama-type congenital muscular dystrophy. *Nature*, **394**, 388–392.

21. Roscioli, T., Kamsteeg, E.J., Buysse, K., Maystadt, I., van Reeuwijk, J., van den Elzen, C., van Beusekom, E., Riemersma, M., Pfundt, R., Vissers, L.E.L.M. *et al.* (2012) Mutations in ISPD cause Walker–Warburg syndrome and defective glycosylation of α-dystroglycan. *Nat. Genet.*, **44**, 581–585.
22. Willer, T., Lee, H., Lommel, M., Yoshida-Moriguchi, T., Beltrán-Valero de Bernabé, D., Venzke, D., Cirak, S., Schachter, H., Vajsar, J., Voit, T. *et al.* (2012) ISPD loss-of-function mutations disrupt dystroglycan O-mannosylation and cause Walker–Warburg syndrome. *Nat. Genet.*, **44**, 575–580.
23. Manzini, M.C., Tambunan, D.E., Hill, R.S., Yu, T.W., Maynard, T.M., Heinzen, E.L., Shianna, K.V., Stevens, C.R., Partlow, J.N., Barry, B.J. *et al.* (2012) Exome sequencing and functional validation in zebrafish identify GTDC2 mutations as a cause of Walker–Warburg syndrome. *Am. J. Hum. Genet.*, **91**, 541–547.
24. Lefeber, D.J., Brouwer, A.P., Morava, E., Riemersma, M., Schuurs-Hoeijmakers, J.H., Absmanner, B., Verrijp, K., Akker, W.M., Huijben, K., Steenbergen, G. *et al.* (2011) Autosomal recessive dilated cardiomyopathy due to DOLK mutations results from abnormal dystroglycan O-mannosylation. *PLoS Genet.*, **7**, e1002427.
25. Lefeber, D.J., Schonberger, J., Morava, E., Guillard, M., Huyben, K.M., Verrijp, K., Grafakou, O., Evangeliou, A., Preijers, F.W., Manta, P. *et al.* (2009) Deficiency of Dol-P-Man synthase subunit DPM3 bridges the congenital disorders of glycosylation with the dystroglycanopathies. *Am. J. Hum. Genet.*, **85**, 76–86.
26. Barone, R., Aiello, C., Race, V., Morava, E., Foulquier, F., Riemersma, M., Passarelli, C., Concolino, D., Carella, M., Santorelli, F. *et al.* (2012) DPM2-CDG: A muscular dystrophy–dystroglycanopathy syndrome with severe epilepsy. *Ann. Neurol.*, **72**, 550–558.
27. Manya, H., Chiba, A., Yoshida, A., Wang, X., Chiba, Y., Jigami, Y., Margolis, R.U. and Endo, T. (2004) Demonstration of mammalian protein O-mannosyltransferase activity: Coexpression of POMT1 and POMT2 required for enzymatic activity. *Proc. Natl Acad. Sci. U.S.A.*, **101**, 500–505.
28. Inamori, K.I., Yoshida-Moriguchi, T., Hara, Y., Anderson, M.E., Yu, L. and Campbell, K.P. (2012) Dystroglycan function requires xylosyl- and glucuronyltransferase activities of LARGE. *Science*, **335**, 93–96.
29. Ibraghimov-Beskrovnaya, O., Ervasti, J.M., Leveille, C.J., Slaughter, C.A., Sernett, S.W. and Campbell, K.P. (1992) Primary structure of dystrophin-associated glycoproteins linking dystrophin to the extracellular matrix. *Nature*, **355**, 696–702.
30. Hara, Y., Balci-Hayta, B., Yoshida-Moriguchi, T., Kanagawa, M., Beltrán-Valero de Bernabé, D., Gündeşli, H., Willer, T., Satz, J.S., Crawford, R.W., Burden, S.J. *et al.* (2011) A dystroglycan mutation associated with limb-girdle muscular dystrophy. *N. Engl. J. Med.*, **364**, 939–946.
31. Bao, X., Kobayashi, M., Hatakeyama, S., Angata, K., Gullberg, D., Nakayama, J., Fukuda, M.N. and Fukuda, M. (2009) Tumor suppressor function of laminin-binding α-dystroglycan requires a distinct β3-N-acetylglucosaminyltransferase. *Proc. Natl. Acad. Sci. U.S.A.*, **106**, 12109–12114.
32. Godfrey, C., Foley, A.R., Clement, E. and Muntoni, F. (2011) Dystroglycanopathies: coming into focus. *Curr. Opin. Genet. Dev.*, **21**, 278–285.
33. Sasaki, K., Kurata-Miura, K., Ujita, M., Angata, K., Nakagawa, S., Sekine, S., Nishi, T. and Fukuda, M. (1997) Expression cloning of cDNA encoding a human β-1,3-N-acetylglucosaminyltransferase that is essential for poly-N-acetyllactosamine synthesis. *Proc. Natl Acad. Sci. U.S.A.*, **94**, 14294–14299.
34. Hu, Y., Li, Z.F., Wu, X. and Lu, Q. (2011) Large induces functional glycans in an O-mannosylation dependent manner and targets GlcNAc terminals on alpha-dystroglycan. *PLoS One*, **6**, e16866.
35. Woods, C.G., Cox, J., Springell, K., Hampshire, D.J., Mohamed, M.D., McKibbin, M., Stern, R., Raymond, F.L., Sandford, R., Malik Sharif, S. *et al.* (2006) Quantification of homozygosity in consanguineous individuals with autosomal recessive disease. *Am. J. Hum. Genet.*, **78**, 889–896.
36. Rodriguez-Rigueiro, T., Valladares-Ayerbes, M., Haz-Conde, M., Blanco, M., Aparicio, G., Fernandez-Puente, P., Blanco, F.J., Lorenzo, M.J., Aparicio, L.A. and Figueroa, A. (2011) A novel procedure for protein extraction from formalin-fixed paraffin-embedded tissues. *Proteomics*, **11**, 2555–2559.
37. Parsons, M.J., Campos, I., Hirst, E.M.A. and Stemple, D.L. (2002) Removal of dystroglycan causes severe muscular dystrophy in zebrafish embryos. *Development*, **129**, 3505–3512.
38. Lin, Y.Y., White, R.J., Torelli, S., Cirak, S., Muntoni, F. and Stemple, D.L. (2011) Zebrafish fukutin family proteins link the unfolded protein response with dystroglycanopathies. *Hum. Mol. Genet.*, **20**, 1763–1775.